原 著

院内感染事例での潜在性結核感染治療（予防内服）前のCTスクリーニングの有用性

西井研治[*1]、玉置明彦[*1]、小谷剛士[*1]、三宅俊嗣[*1]
朝倉里都子[*1]、沼田健之[*1]、守谷欣明[*1]、宮木功次[*2]

胸部CT検診は肺癌の早期発見を目的に発展を遂げてきたが、肺結核も早期発見されるとの報告もみられている。今回、結核感染高危険群に対して、胸部CT検診の有用性を検討した。

2008年10月から11月にかけてA病院へ肺炎疑いで入院していた90歳男性患者が、多量排菌の結核患者であったことが判明し、院内で接触者検診が行われた。接触が疑われた職員31人にQFT（QuantiFERON TB-2G）と胸部X-Pが施行され、QFT陽性および疑陽性者9人のうち同意の得られた8人に2009年3月CTスクリーニングを行った。

胸部X-Pは31人全員以上を認めなかった。QFT陽性（ESAT-6, CFP-10 が0.35 IU/ml以上）は5人で、全員CTスクリーニングを受け、ESAT-6：0.74 IU/mlの50歳看護師にCTで右S6に小粒状影（acinar pattern, tree-in bud）を認め、活動性結核と診断した。QFT疑陽性（ESAT-6, CFP-10 が0.1 IU/ml～0.35 IU/ml未満）は4人で、3例がCTスクリーニングを受け、ESAT-6：0.18 IU/ml、CFP-10：0.16 IU/mlの27歳看護師がCTで右S2に小粒状影（acinar pattern）を認め、活動性結核と診断された。肺結核を発症していた2例はINH + REF + EB + PZAによる標準治療を施行した。発病が否定された7例に対してはINH単剤による予防内服を行った。

今回のCTスクリーニングで発見された活動性結核は、胸部X-Pでは指摘できず、通常の検診ではINH単剤の予防内服が指示されて、治療失敗およびINH耐性化をきたした可能性もあり、CTスクリーニングの有用性が証明された。

キーワード： 胸部CTスクリーニング、QFT（QuantiFERON TB-2G）、潜在性肺結核
J Thorac CT Screen 2010；17：145-149

はじめに

保健所で行われている結核接触者検診で、感染が強く疑われるが胸部X-Pが正常であったために潜在結核感染の治療を受け、のちにイソニコチン酸ヒドラジド（INH）耐性結核を発病した例が報告されている[1]。すでに発病している患者に対して、あやまって1剤治療を行ったために耐性結核となったと推定される。胸部X-Pでは発見されなかったが、CTでスクリーニングを行うことで結核発病が発見できたという報告[2]や、小児の濃厚接触者に対してCTを施行し、発病者を早期に見つけた報告[3]もある。しかし、成人の接触者検診でCTによるスクリーニングをどのように実施するかについては、コンセンサスが得られていないが、QFTの接触者検診への積極的導入の推奨が打ち出されて[4]、結核菌感染者の絞り込みが可能になったことをふまえて、今回の研究を計画した。

[*1] 岡山県健康づくり財団附属病院
〒700-0952 岡山市北区平田408-1
nkenji@okakenko.jp
[*2] 赤磐医師会病院外科

対象と方法

2008年10月から11月にかけてA病院へ肺炎疑いで入院していた90歳男性患者が、多量排菌の結核患者であったことが判明し、接触者検診を計画した。接触が確認された職員31人にQFTと胸部X-Pを施行、QFT陽性および疑陽性者9人のうち同意の得られた8人に2009年3月CTスクリーニングを行った。

QFT検査の実施方法は、全血5 ccをヘパリン採血し、12時間以内に結核菌特異タンパクであるESAT-6およびCFP-10で刺激し、16～24時間インキュベートする。同時に生理食塩水、マイトジェンに対する応答も測定する。インターフェロンγをELISA法によって測定し、インターフェロンγ量は、抗原、PHA刺激下での測定値から陰性対照での測定値を引き算して求める方法をとった。

胸部CT撮影は、SIEMENS Emotion16で、管電圧：130 kV、管電流：AUTO、テーブルピッチ：0.8、コリメーション：1.2 mm×16、再構成間隔：8 mmの条件で行った。今回の検診は、通常撮影モードで行い、低線量CTでは撮影していない。

結核の専門家でつくる感染症対策委員会において、QFT値の評価・CT検診フィルムの判定および治療方針を決定した。

表1　接触者検診結果

性別	年齢	Nil	ESAT-6	CFP-10	Mitogen	E-N	C-N	M-N	判定
男	37	0.08	0.05	0.06	15.28	−0.03	−0.02	15.20	陰性
男	26	0.12	0.15	0.14	15.28	0.03	0.02	15.16	陰性
女	46	0.07	0.37	0.06	6.65	0.30	−0.01	6.58	疑陽性
女	50	0.31	1.05	0.30	15.28	0.74	−0.01	14.97	陽性
女	44	0.07	0.07	0.06	15.28	0.00	−0.01	15.21	陰性
女	25	0.04	0.04	0.05	15.28	0.00	0.01	15.24	陰性
女	51	0.17	0.09	0.08	15.28	−0.08	−0.09	15.11	陰性
女	45	0.10	0.10	0.10	15.28	0.00	0.00	15.18	陰性
女	48	0.05	0.14	0.05	15.28	0.09	0.00	15.23	陰性
女	46	0.04	0.04	0.04	15.28	0.00	0.00	15.24	陰性
女	23	0.27	0.59	0.62	15.28	0.32	0.35	15.01	陽性
女	40	0.89	1.03	1.73	15.28	0.14	0.84	14.39	陽性
女	47	0.12	0.14	0.12	9.54	0.02	0.00	9.42	陰性
男	61	0.05	0.07	0.06	15.61	0.02	0.01	15.56	陰性
女	56	0.08	0.06	0.10	15.61	−0.02	0.02	15.53	陰性
女	27	9.52	15.61	3.86	15.61	6.09	−5.66	6.09	陽性
女	56	0.22	0.20	0.21	15.61	−0.02	−0.01	15.39	陰性
女	27	0.05	0.23	0.21	15.61	0.18	0.16	15.56	疑陽性
女	35	0.13	0.43	0.47	15.61	0.30	0.34	15.48	疑陽性
女	54	0.18	0.17	0.21	15.61	−0.01	0.03	15.43	陰性
女	38	0.07	0.06	0.07	15.61	−0.01	0.00	15.54	陰性
女	37	0.44	0.06	0.06	15.61	−0.38	−0.38	15.17	陰性
男	35	0.04	0.04	0.05	15.61	0.00	0.01	15.57	陰性
女	53	0.14	0.12	0.16	18.66	−0.02	0.02	18.52	陰性
女	42	0.13	0.18	0.37	18.66	0.05	0.24	15.53	疑陽性
男	23	0.06	0.05	0.05	18.66	−0.01	−0.01	18.60	陰性
女	32	0.08	0.13	0.08	14.92	0.05	0.00	14.84	陰性
男	40	0.05	0.06	0.06	16.26	0.01	0.01	16.21	陰性
女	33	0.36	0.42	0.34	16.26	0.06	−0.02	15.90	陰性
女	62	0.28	5.37	2.34	16.26	5.09	2.06	15.98	陽性

結　果

胸部X-PとQFTは31人に行い、胸部X-Pは全員異常を認めなかった。QFTは5人が陽性（ESAT-6またはCFP-10 が0.35 IU/ml以上）、4人が疑陽性であった（**表1**）。陽性者5人全員がCTスクリーニングを受け、ESAT-6：0.74 IU/mlの50歳看護師にCTで右S6に小粒状影（acinar pattern, tree- in bud）を認め、活動性結核と診断した（**図1**）。QFT疑陽性（ESAT-6, CFP-10 が0.1 IU/ml ～0.35 IU/ml未満）は4人で、CTを拒否した1例を除いた3例がCTスクリーニングを受け、ESAT-6：0.18 IU/ml, CFP-10：0.16 IU/mlの27歳看護師がCTで右S2に小粒状影（acinar pattern）を認め、活動性結核と診断した（**図2**）。QFT陽性であった23歳看護師も浸潤影を認めたが、無治療で陰影が改善したため、非特異的炎症と判断した。肺結核を発症していた2例はINH + REF + EB + PZAによる標準治療を施行した。発病が否定された7例に対してはINH単剤による予防内服を行った。発病していた2例は、いずれも6カ月の治療終了後に陰影はほとんど消失した。予防内服した、CT拒否者も含む7例に発病者はみられていない。

考　察

わが国では、結核の集団感染事件の多くが医療機関で発生しており、医療従事者の潜在性結核感染への対策は重要である[5]。今回の事例のように、肺炎として入院して肺結核とのちに判明して、大きな問題になるのが多いと思われる。わが国では結核菌の感染機会があり、胸部X-Pで発病が確認できない場合、INH単剤での予防内服が行われており、一定の発病予防効果が認められている[6, 7]。しかし、INH投与中や投与終了後に活動性結核が発症する例も報告されており[8]、その原因として、胸部X-P撮影時にすでに結核が発症しており、それに気付かぬまま、単剤での治療を行ったためではないかと考えら

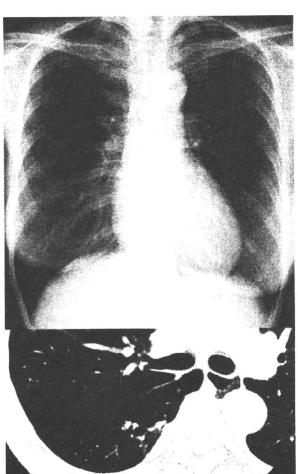

図1　結核発症ケース（50歳　看護師）

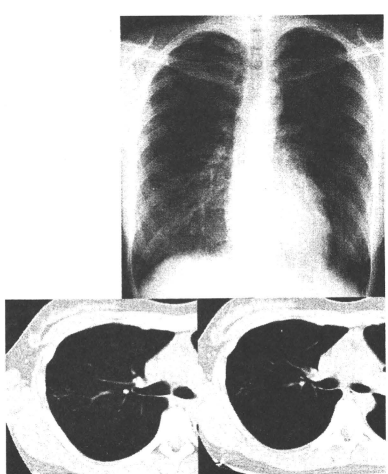

図2　結核発症ケース（27歳　看護師）

れている。豊田は、「発病者が多発する場合には、軽度の発病を見逃さないために，濃厚接触者の化学予防開始時には、CT などの精査も考慮すべき」[1]と考察している。このようにCTを精査と考えるのが一般的であったが、低線量CT検診が普及している現在の状況では、スクリーニングととらえてよいのではないかと思われる。

その他、単純胸部X-Pでは見つからなかった病変がCT で見つかった例としては、韓国における89 名の発病者を出した集団感染事例において12 例のCT 発見例が見られている[2]。この例では、胸部X-PおよびツベルクリンCT検査の後、ツベルクリン反応陽性者にQFT-G を行い、QFT-G陽性者とツベルクリン反応15 mm 以上の接触者に対してCT 撮影を行って12 名の発病者を発見したもので、ツベルクリン反応を条件にしていることを除けば、我々が行ったCTスクリーニングの方式と似ている。しかしCT 所見についての詳細な分析は行われていないため、今回の我々の検討で、結核の初期画像が詳細の明らかにできた意義は大きいと考えられる。問題点として、他の報告例と同様に、今回のCT撮影条件が低線量でなかったことがあげられる。今後、潜在性結核感染疑い者にCTスクリーニングを広げていく上で、低線量CTでも結核初期病変を十分指摘できることを証明する必要があり、今後の研究課題にしたい。

結　語

今回の検討で、CTで発見された活動性結核は、胸部X-Pでは指摘できず、通常の検診ではINH単剤の予防内服が指示されて、治療失敗およびINH耐性化をきたした可能性もあり、CTスクリーニングの有用性が示唆された。

文　献

[1] 豊田　誠、森岡茂治：化学予防中にINH 耐性で発病した結核患者. 結核. 2001 ; 76 : 663-666
[2] Lew WJ : TB outbreak in a school in Korea. 1st Asian Pacific Region conference 2007 of International Union Against Tuberculosis and Lung Diseases, Asian Pacific Region conference secretariat, Kuala Lumpur. 2007, 52
[3] 片倉茂樹、今川智之、伊藤秀一、他：胸部単純X 線写真では所見なく、胸部CT スキャンにて診断された小児肺結核症. 感染症学雑誌. 1999; 73: 130-137
[4] 日本結核病学会予防委員会：結核の院内感染対策について. 結核. 1998; 73: 95-100
[5] 青木正和：結核の院内感染、改訂版. 結核予防会. 東京. 1998
[6] 千葉保之、高原　義、他：化学予防の遠隔成績について（その10年間の観察）東鉄健康管理所報10：138-154.1966
[7] Lincoln EM: The effect of antimicrobial therapy on the prognosis of primary tuberculosis in children. Am Rev Tuberc 69: 682-689. 1954
[8] 池田一成、杉森光子、川崎一輝、他：INH予防内服にもかかわらず発病した小児結核の検討. 結核. 1992 ; 67 :653-658

CT Screening before Treatment of Latent Tuberculous Infection for the Diagnosis of Clinical TB among Contacts

Kenji Nishii[*1], Akihiko Tamaoki[*1], Tsuyoshi Kodani[*1], Toshitsugu Miyake[*1]
Ritsuko Asakura[*1], Takeyuki Numata[*1], Yoshiaki Moritani[*1], Kouji Miyagi[*2]

[*1] Okayama Health Foundation Hospital
[*2] Akaiwa Ishikai Hospital, department of surgery

Abstract

Until now, patient suspected of having latent tuberculosis infection has chest X-ray examination to exclude clinical tuberculosis. But we sometimes misdiagnosed clinical tuberculosis as latent tuberculosis by chest X-ray only. Recently, some reports have pointed out that CT scan can detect early clinical tuberculosis in incorrect latent tuberculosis by chest X-ray. Therefore, to evaluate the value of CT screening for the detection of clinical tuberculous diseases among persons who are suspected to be infected at the contact examination, we performed CT screening on QuantiFERON-TB-2G (QFT) positive participants in hospital tuberculosis infection.

A 90-year-old man of tuberculosis had been in the A hospital from Oct. through Nov., who was misdiagnosed with pneumonia. After the correct diagnosis, contact examination of tuberculosis was performed to 31 participants suspected of transmission. All of them were with normal chest X-rays findings. And 5 cases among 31 participants with a positive QFT test had CT screening, and one patient having clinical tuberculosis was found. In indeterminant case, one nurse of tuberculosis was detected by CT scan. These patients of tuberculosis received standard chemotherapy, and cured.

In the result, CT screening should be considered for the detection of clinical tuberculosis cases among contacts.

Key words: CT, Clinical TB, QuantiFERON-TB-2G, Latent tuberculous infection
J Thorac CT Screen 2010;17:145-149

Biochemical and Biophysical Research Communications 393 (2010) 201–206

Contents lists available at ScienceDirect

Biochemical and Biophysical Research Communications

journal homepage: www.elsevier.com/locate/ybbrc

MKP-7, a JNK phosphatase, blocks ERK-dependent gene activation by anchoring phosphorylated ERK in the cytoplasm

Kouhei Masuda [a,b,1], Chiaki Katagiri [a,b], Miyuki Nomura [a], Masami Sato [a,c], Kyoko Kakumoto [d], Tsuyoshi Akagi [d,e], Kunimi Kikuchi [b], Nobuhiro Tanuma [a], Hiroshi Shima [a,*]

[a] Division of Cancer Chemotherapy, Miyagi Cancer Center Research Institute, Natori, Japan
[b] Division of Biochemical Oncology and Immunology, Institute for Genetic Medicine, Hokkaido University, Sapporo, Japan
[c] Thoracic Surgery, Miyagi Cancer Center, Natori, Japan
[d] Laboratory of Molecular Oncology, Osaka Bioscience Institute, Osaka, Japan
[e] Kan Research Institute, Kobe, Japan

ARTICLE INFO

Article history:
Received 19 January 2010
Available online 1 February 2010

Keywords:
Dual-specificity protein phosphatase
MKP-7
ERK
JNK
Anchor protein

ABSTRACT

MAPK phosphatase-7 (MKP-7) was identified as a JNK-specific phosphatase. However, despite its high specificity for JNK, MKP-7 interacts also with ERK. We previously showed that as a physiological consequence of their interaction, activated ERK phosphorylates MKP-7 at Ser-446, and stabilizing MKP-7. In the present study, we analyzed MKP-7 function in activation of ERK. A time-course experiment showed that both MKP-7 and its phosphatase-dead mutant prolonged mitogen-induced ERK phosphorylation, suggesting that MKP-7 functions as a scaffold for ERK. An important immunohistological finding was that nuclear translocation of phospho-ERK following PMA stimulation was blocked by co-expressed MKP-7 and, moreover, that phospho-ERK co-localized with MKP-7 in the cytoplasm. Reporter gene analysis indicated that MKP-7 blocks ERK-mediated transcription. Overall, our data indicate that MKP-7 down-regulates ERK-dependent gene expression by blocking nuclear accumulation of phospho-ERK.

Introduction

Cells often respond to environmental cues and physiological stimuli—such as growth factors, hormones, cytokines, and stress such as osmotic shock, radiation, and ischemic injury—by activating mitogen-activated protein kinases (MAPKs) [1]. Five MAPK pathways have been identified in eukaryotic cells, three of which are relatively well characterized: the extracellular signal-regulated kinase (ERK) pathway, the c-Jun amino-terminal kinase (JNK) pathway, and the p38 pathway. MAPKK is a dual-specificity protein kinase that phosphorylates tyrosine and threonine residues in a TXY motif of MAPK, leading to full MAPK activation. In general, activation of the ERK cascade leads to cell proliferation, differentiation, or enhanced cell survival after cellular stress. However, activation of the JNK and p38 cascades is usually associated with enhanced apoptosis and production of inflammatory cytokines [2].

ERK pathway components must be tightly controlled in terms of both signal duration and subcellular localization. These responses are regulated via ERK-dependent phosphorylation of cytoplasmic proteins such as p90 ribosomal S6 kinase 1 (RSK1) and several nuclear proteins including the transcription factor Elk-1 [3]. ERK1/2 are distributed throughout the cytoplasm of quiescent cells, but upon stimulation, a significant population of ERK1/2 accumulates in the nucleus [4]. While the mechanism involved in nuclear accumulation of ERK1/2 remains elusive, nuclear retention, dimerization, phosphorylation, and release from cytoplasmic anchors have been shown to play a role [4].

MAPK phosphatases (MKPs) are dual-specificity protein phosphatases that down-regulate MAPK activity by dephosphorylating the TXY motif [5]. To date, 10 MKPs have been reported in mammalian cells, and they are precisely regulated in their substrate specificity to avoid inappropriate MAPK inactivation [5]. MKPs are primarily composed of two domains, a rhodanese-like domain and a dual-specificity phosphatase catalytic domain. By phylogenetic analysis, MKPs are classified into three subgroups [6]. Subgroup I contains the nuclear MKPs: MKP-1/DUSP1, PAC1/DUSP2, MKP-2/DUSP4, and VH3/DUSP5, which target the three primary MAPKs—ERK, JNK and p38. Subgroup II includes cytoplasmic

Abbreviations: MAP, mitogen-activated protein; ERK, extracellular signal-regulated kinase; JNK, c-Jun N-terminal kinase; MEK, MAP kinase/ERK kinase; DSP, dual-specificity phosphatase; MKP, MAP kinase phosphatase; HA, hemagglutinin; PBS, phosphate-buffered saline; PMA, 12-O-tetradecanoylphorbol-13-acetate; EGF, epidermal growth factor; FBS, fetal bovine serum; CTS, COOH-terminal stretch; RSK1, p90 ribosomal S6 kinase 1; SRE, serum responsive element; Luc, luciferase

* Corresponding author. Address: Division of Cancer Chemotherapy, Miyagi Cancer Center Research Institute, 47-1 Nodayama, Medeshima-Shiode, Natori 981-1293, Japan. Fax: +81 22 381 1196.
E-mail address: shima-hi632@pref.miyagi.jp (H. Shima).
[1] Present address: Department of Cancer and Cell Biology, Metabolic Diseases Institute, University of Cincinnati, Cincinnati, OH 45237, USA.

0006-291X/$ - see front matter © 2010 Elsevier Inc. All rights reserved.
doi:10.1016/j.bbrc.2010.01.097

MKPs: MKP-3/DUSP6, PYST2/DUSP7 and MKP-4/DUSP9, which mainly target ERK, and MKP-5/DUSP10, which targets JNK and p38. Subgroup III consists of the nuclear and cytoplasmic MKPs, MKP-7/DUSP16 and VH5/DUSP8, both of which mainly dephosphorylate JNK.

MKP-7, a JNK-specific phosphatase, exhibits a unique COOH-terminal stretch (CTS) in addition to the MKP common structure [7,8]. Previously, we demonstrated that MKP-7 binds ERK2 as well as JNK1, despite its high specificity towards JNK1 as a substrate [7]. This observation suggested an unidentified function underlying interaction of MKP-7 with ERK2. We then found that the MKP-7 CTS domain is bound by ERK, and that activated ERK phosphorylates Ser-446 in the CTS, stabilizating MKP-7 [9,10].These results indicate that activation of the ERK pathway strongly blocks JNK activation by phosphorylation-mediated stabilization of MKP-7. Here, we asked whether MKP-7 regulates the ERK pathway by interacting ERK proteins. Time-course analysis of ERK activation showed that MKP-7 induced enhanced and prolonged ERK phosphorylation, suggesting a scaffold function. Immunological analyses showed that phospho-ERK2 co-localizes with MKP-7 and accumulates in the cytoplasm. These observations reveal a novel role for MKP-7 as a cytoplasmic anchor protein that prevents nuclear targeting of phospho-ERK.

Materials and methods

Expression vectors. pFLAG-MKP-7, pFLAG-MKP-7CS (C244S) and pFLAG-MKP-2 have been described [7,10]. To construct pCX4-bleo-RSK1, full length human RSK1 cDNA was amplified by PCR from a cDNA library prepared with mRNA of human fibroblast MRC5, and subcloned into *Eco*RI site of pCX4-bleo [11]. pCMV-b-galactosidase has been described [12], pSRE-Luc and pAP-1-Luc were from Stratagene (Garden Grove, CA, USA) and pSRα-HA-ERK2 was a gift from Dr. M. Karin (University of California, San Diego).

Cell culture, DNA transfection and stimulation. HeLa and COS-7 cells were maintained in Dulbecco's modified Eagle's medium (DMEM) containing 10% fetal bovine serum (FBS) at 37 °C under 5% CO_2. Cells were co-transfected with various pFLAG-MKP-7 expression vectors together with pSRα-HA-ERK2. For transient assays, cells were transfected using the Fugene-6 transfection reagent (Roche Diagnostics Inc., Manheim, Germany) according to the manufacturer's recommendation. Eighteen hours later, cells were starved 18 h and then exposed to 100 ng/ml human EGF (Sigma Chemical Co, St. Louis, MO, USA) or 10 ng/ml PMA (Sigma) for indicated times. For 10 μM U0126 treatment (Promega, Madison, WI, USA), transfected cells were exposed to the compound for 1 h before stimulation.

Detection of expressed proteins. Preparation of cell lysates was described previously [7]. Each sample was separated by a SDS–polyacrylamide gel electrophoresis (SDS–PAGE) on 7.5% or 10% gels and transferred to a nitrocellulose membrane. Expression levels of HA-tagged ERK and FLAG-tagged MKPs were monitored using anti-HA (12CA5) (Roche) and anti-FLAG M2 (Sigma) monoclonal antibodies, respectively. ERK2 activation was monitored by an anti-phospho-ERK1/2 antibody (Thr202/Tyr204) (Cell Signaling Technology Inc., Danvers, MA, USA). The amount and activation of RSK1 were monitored using anti-RSK (BD, Franklin Lakes, NJ, USA) and anti-phospho-p90RSK (Thr-359/Ser-363) (Cell Signaling) antibodies, respectively. Signals were detected by enhanced chemiluminescence using the ECL reagent (Amersham Pharmacia Biotech, Piscataway, NJ, USA).

Cell staining. HeLa cells on coverslips coated with VITROGEN 100 (Collagen Biochemical, Palo Alto, CA, USA) were co-transfected with various pFLAG-MKP-7 expression vectors together with pSRα-HA-ERK2. Transfected cells were fixed in PBS containing 3.7% formaldehyde for 10 min and then permeabilized with PBS containing 0.5% Triton X-100 for 5 min. After incubation in PBS containing 3% BSA (PBS-B) for 2 h, cells were incubated with anti-FLAG M2 antibody or anti-FLAG polyclonal antibody (provided from Dr. K. Yamashita, Kanazawa University) to detect FLAG-tagged proteins and with anti-HA antibody to detect HA-tagged proteins in PBS-B overnight at 4 °C. After three PBS washes, cells were incubated for 20 min at 37 °C with Cy3-conjugated goat anti-mouse IgG + IgM (H + L) antibody (CHEMICON International, Temecula, CA, USA), AlexaFluor 488-conjugated goat anti-mouse IgG (H + L) antibody (Molecular Probes, Eugene, OR, USA), AlexaFluor 488-conjugated goat anti-rabbit IgG (H + L) (Molecular Probes), or AlexaFluor 546-conjugated goat anti-rabbit IgG (H + L) (Molecular Probes) in PBS-B. After three PBS washes, coverslips were mounted with PBS containing 90% glycerol. Fluorescence was visualized using a fluorescence microscope.

Reporter analysis. HEK293 cells were transfected with pSRE-Luc or pAP-1-Luc together with pCMV-b-galactosidase and MKP expression vectors. Eighteen hours later, cells were serum-starved for 12 h, and then treated with 10 ng/ml PMA. Six hours later, cells were harvested and washed with PBS (−) twice and then lysed with LCb lysis buffer (Toyo Ink, Tokyo, Japan). Cell lysates were obtained by one freeze–thaw treatment and centrifuged. Luciferase activity in lysates was measured with Picagene (Toyo ink) using MicroLumat Plus LB96 V (Belthold, Bad Wildbad, Germany). Luciferase activities were normalized to activity of co-expressed b-galactosidase, which was assayed as described [12].

Results

MKP-7 induces enhanced and prolonged EGF-stimulated ERK phosphorylation

We compared the time-course of EGF-stimulated ERK in the presence of MKP-7 in COS-7 cells. (Fig. 1A). Phosphorylation levels of HA-ERK2 reached maximal levels 15 min after EGF stimulation, and decreased to basal levels by 60 min (Fig. 1A). However, interestingly, when FLAG-MKP-7 was co-expressed, we observed enhanced and prolonged phosphorylation of HA-ERK2 (Fig. 1A). By contrast, as shown in Fig. 1B, co-expression of MKP-2 completely suppressed ERK activation until 90 min after EGF treatment. These results indicate that FLAG-MKP-7, a JNK-specific phosphatase, upregulates ERK phosphorylation.

MKP-7 catalytic activity is not required to induce enhanced and prolonged ERK phosphorylation

To determine whether MKP-7 phosphatase activity is required to induce enhanced and prolonged ERK phosphorylation, COS-7 cells were co-transfected with pSRα-HA-ERK2 together with pFLAG-CMV2, pFLAG-MKP-7 or pFLAG-MKP-7CS, which lacks phosphatase activity (Fig. 1C). Following EGF treatment, transfected cells were incubated for the indicated times, and phosphorylation levels of HA-ERK2 were examined. As shown in Fig. 1C, phosphorylation levels of HA-ERK2 after EGF stimulation were up-regulated in the presence of both MKP-7 and MKP-7CS. A similar effect was also seen following PMA stimulation (data not shown). These data show that MKP-7 enhances and prolongs PMA- or EGF-stimulated ERK phosphorylation, and that this effect does not require enzyme activity of MKP-7.

MKP-7 anchors phosphorylated ERK in the cytoplasm

Following mitogenic stimulation, ERK1/2 is phosphorylated, dimerizes, translocates to the nucleus, and returns to the cytoplasm when it is dephosphorylated [4]. To determine how MKP-7 induces

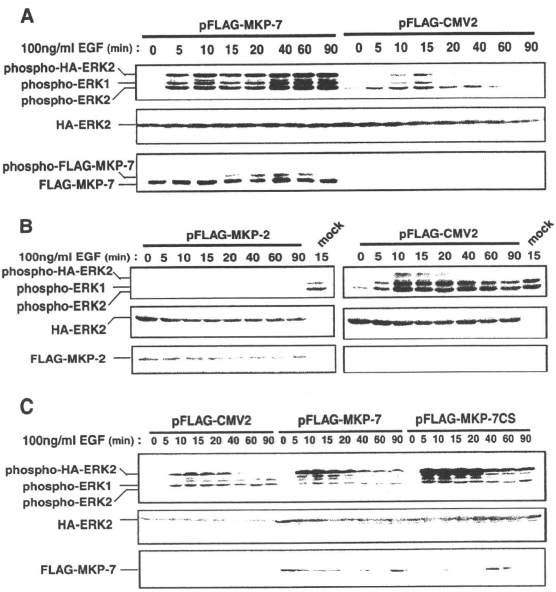

Fig. 1. MKP-7 induces enhanced and prolonged EGF-stimulated ERK phosphorylation. COS-7 cells were transfected with 1.2 μg of pFLAG-MKP-7 or pFLAG-CMV2 together with 0.6 μg of pSRα-HA-ERK2 (A). COS-7 cells were transfected with 1.2 μg of pFLAG-MKP-2 or pFLAG-CMV2 together with 0.6 μg of pSRα-HA-ERK2 (B). COS-7 cells were co-transfected with 0.6 μg of pSRα-HA-ERK2 together with 1.2 μg pFLAG-CMV2, pFLAG-MKP-7, or pFLAG-MKP-7CS (C). Eighteen hours later, cells were starved for 18 h and stimulated with 100 ng/ml EGF for indicated periods. Expressed proteins were separated on 7.5% SDS–PAGE and analyzed by immunoblot using anti-phospho-ERK1/2, anti-HA and anti-FLAG antibodies, respectively. Data represent three independent experiments.

up-regulated ERK phosphorylation in cells, we asked whether MKP-7 functions in ERK localization by analyzing time-dependent subcellular distribution of HA-ERK2 in the absence (Fig. 2A) or presence (Fig. 2B) of FLAG-MKP-7. Immunostaining with anti-HA antibody showed that HA-ERK2 was localized in the cytoplasm (at 0 min), in both the cytoplasm and nucleus (at 10 min), primarily in the nucleus (at 30 min), and in the cytoplasm and nucleus (at 60 min) after PMA treatment (Fig. 2A, middle). Analysis of immunostaining with an anti-phospho-ERK1/2 antibody showed that phosphorylated HA-ERK2 was only nuclear (Fig. 2A, left). In a striking contrast, when FLAG-MKP-7 was co-expressed, HA-ERK2 was detected only in the cytoplasm, even after PMA stimulation, and HA-ERK2 localization was almost identical to that of FLAG-MKP-7 (Fig. 2B, right). Note that in FLAG-MKP-7 expressing cells phosphorylated HA-ERK2 was not detected in the nucleus but instead co-localized with cytoplasmic FLAG-MKP-7 (Fig. 2C). In cells in which FLAG-MKP-7 was not co-expressed, endogenous phospho-ERK1/2 was detected in the nucleus (Fig. 2C). These data strongly suggest that MKP-7 functions to anchor phospho-ERK1/2 in the cytoplasm and prevent its nuclear accumulation.

MKP-7 does not enhance ERK-dependent RSK1 phosphorylation

When FLAG-MKP-7 was co-expressed, phospho-HA-ERK2 accumulated in the cytoplasm; thus it was possible that ERK substrates in the cytoplasm are highly phosphorylated. We examined this possibility by comparing phosphorylation levels of Thr-359 and Ser-363 of RSK1, a cytoplasmic ERK substrate, in the presence and absence of FLAG-MKP-7. As shown in Fig. 3, sustained HA-ERK2 phosphorylation was detected in FLAG-MKP-7-expressing cells, while enhanced RSK1 phosphorylation at Thr-359 and Ser-363 was not observed. Under the same conditions, the MEK inhibitor U0126 completely suppressed RSK1 phosphorylation (data not shown). These data suggest that, when bound to MKP-7, phospho-ERK does not phosphorylate RSK1 as non-bound phospho-ERK does.

MKP-7 prevents ERK-dependent transcriptional activation

The effect of MKP-7 on JNK- and ERK-dependent transcriptional regulation was analyzed using AP-1- and SRE- driven luciferase reporter constructs (Fig. 4). MKP-2, which similarly dephosphorylates ERK, JNK and p38, inhibited SRE- and AP-1-dependent transcription almost completely. MKP-7 completely inhibited AP-1-dependent gene transcription as expected (Fig. 4A), since MKP-7 efficiently and specifically dephosphorylates JNK [7]. It is noteworthy that MKP-7 suppressed SRE-dependent transcription by 79%, an effect comparable to suppression seen following treatment with 10 μM U0126, a MEK inhibitor (Fig. 4B). Similar inhibition of SRE-dependent transcription was obtained using MKP-7CS

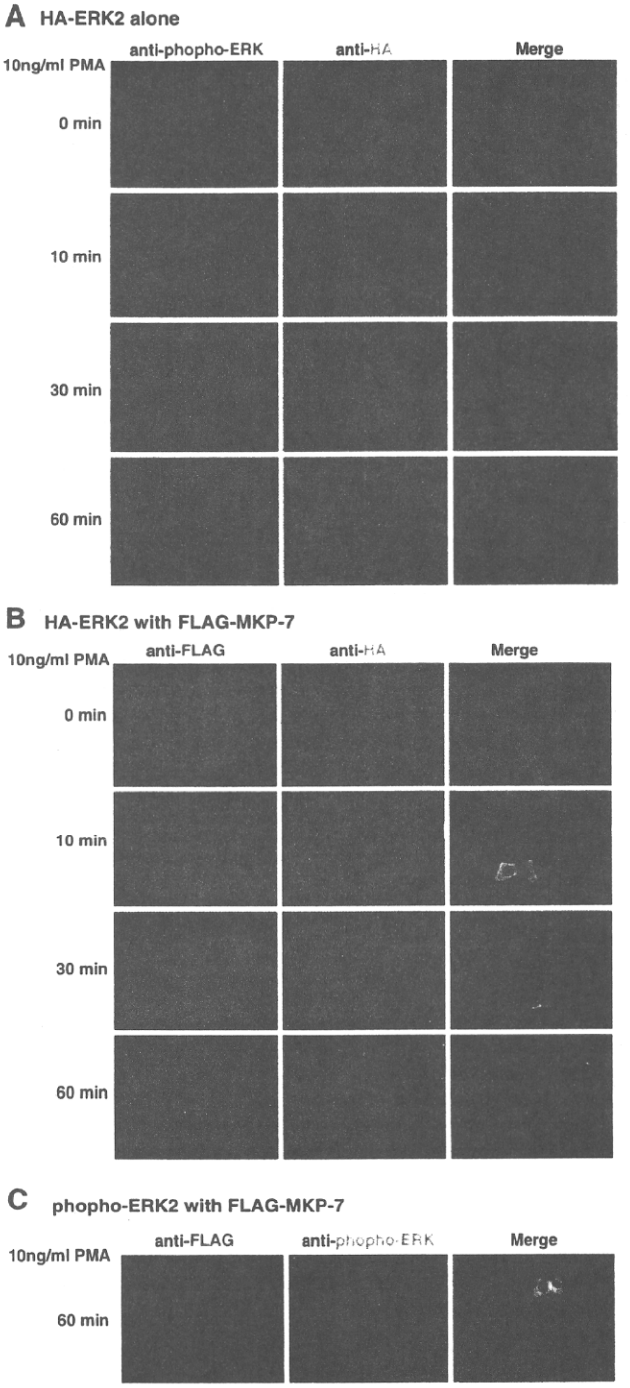

Fig. 2. MKP-7 retains phosphorylated ERK in the cytoplasm. HeLa cells were transfected with 0.6 μg of pSRα-HA-ERK2 with 1.2 μg of pFLAG-CMV (A) or pFLAG-MKP-7 (B). Transfected cells were cultured for 24 h, serum-starved for 18 h, and then cultured with 10 nM PMA for indicated time. (A) Activated ERK was detected by immunofluorescence using an anti-phospho-ERK1/2 rabbit antibody with AlexaFluor 546-conjugated goat anti-rabbit secondary antibody (red). HA-ERK2 was detected by immunofluorescence using an antibody to anti-HA mouse antibody with AlexaFluor 488-conjugated goat anti-mouse antibody (green). (B) FLAG-MKP-7 was detected by immunofluorescence using an anti-FLAG rabbit antibody with AlexaFluor 546-conjugated goat anti-rabbit secondary antibody (red). HA-ERK was detected by immunofluorescence using an antibody to anti-HA mouse antibody with AlexaFluor 488-conjugated goat anti-mouse secondary antibody (green). (C) FLAG-MKP-7 was detected by immunofluorescence using an anti-FLAG mouse antibody with Cy3-conjugated goat anti-mouse secondary antibody (red). Phospho-ERK1/2 was detected by immunofluorescence using an anti-phospho-ERK1/2 rabbit antibody with AlexaFluor 488-conjugated goat anti-rabbit secondary antibody (green). (For interpretation of the references to color in this figure legend, the reader is referred to the web version of this paper.)

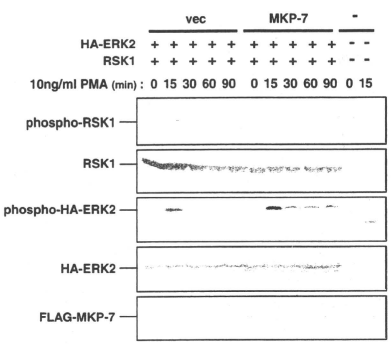

Fig. 3. MKP-7 does not enhance ERK-dependent RSK1 phosphorylation. COS-7 cells were co-transfected with 1.0 μg of either pFLAG-CMV2 or pFLAG-MKP-7 together with 0.5 μg each of pSRα-HA-ERK2 and pCX4-bleo-RSK1. Transfected cells were cultured for 18 h, serum-starved for 18 h, and then treated with 10 ng/ml PMA for indicated time. Phosphorylation and expression levels of RSK1 were detected by anti-phospho-p90RSK (Thr-359/Ser-363) and anti-RSK antibody, respectively. Expression and phosphorylation levels of HA-MAPKs were monitored using anti-HA and anti-phospho-ERK antibodies, respectively. Expression of FLAG-MKP-7 was monitored by anti-FLAG antibody. Data represent three independent experiments.

(Fig. 4B). These results show that MKP-7 down-regulates ERK-dependent transcription and overall support the idea that MKP-7 blocks nuclear accumulation of phospho-ERK.

Discussion

In the present study, we found that MKP-7 and a phosphatase-dead mutant form of the protein induced enhanced and prolonged mitogen-stimulated ERK phophorylation. Immunohistological analysis showed that MKP-7 functions as cytoplasmic anchor for ERK, and importantly that phospho-ERK accumulates in the cytoplasm in the presence of MKP-7. We also analyzed the physiological consequence of blocking nuclear translocation of phospho-ERK. Despite enhanced levels of phospho-ERK, phosphorylation of RSK, a cytoplasmic target, was not enhanced. Importantly, MKP-7 suppressed SRE-driven gene expression to the same level as did treatment with U0126. These observations indicate that MKP-7 inhibits ERK-dependent gene expression by preventing nuclear translocation of phospho-ERK and preventing phospho-ERK from further phosphorylation of RSK1.

Recently, other protein phosphatases have been shown to regulate MAPK localization. Phosphotyrosine phosphatases such as PTP-SL [13], STEP [14] and He-PTP [15] retain ERK in a dephosphorylated form in the cytoplasm by association through the KIM domain and by tyrosine dephosphorylation. MKP-3/DUSP6 was shown to function in cytoplasmic retention of dephosphorylated ERK2 [16]. hVH3/DUSP5 was recently identified as both a phosphatase and nuclear anchor for ERKs [17]. We previously reported that MKP-7 dephosphorylates JNK and localizes it in the cytoplasm in a diffuse cellular distribution [7]. Therefore it is likely that these MAPK phosphatases also function to dephosphorylate and regulate respective MAPKs. By contrast, MKP-7 functions as an anchor protein for ERK rather than a phosphatase, because it retained phospho-ERK2 in the cytoplasm without dephosphorylating it.

Two proteins, PEA-15, and SEF, have been identified as cytoplasmic anchors for ERK2 [18,19]. Both can retain ERK2 in the cytoplasm in the active state, indicating that they may act to restrict ERK2 activity to cytoplasmic targets. By contrast, our data indicates that MKP-7 accumulates phospho-ERK in the cytoplasm but does not lead to enhanced RSK1 phosphorylation. Therefore, MKP-7 interaction might inhibit ERK activation or MKP-7 may occupy the ERK substrate recognition site. As shown here, MKP-7 induced enhanced and prolonged phosphorylation of ERK, and that prolonged phosphorylation was coupled with cytoplasmic scaffold activity as shown in Fig. 2. Since PEA-15 also reportedly induces prolonged ERK phosphorylation, this activity may be a common

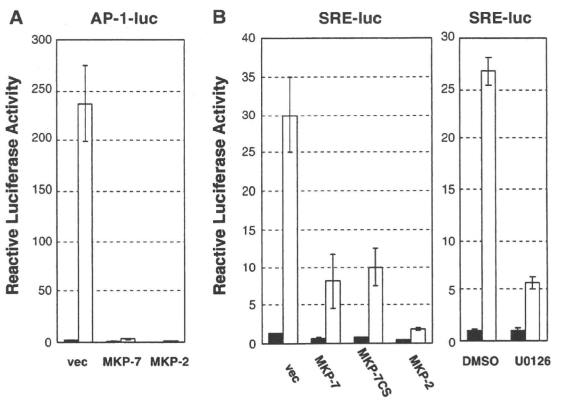

Fig. 4. MKP-7 inhibits transactivation of SRE through the ERK signaling pathway. HEK293 cells in 35-mm dishes were co-transfected with 0.45 μg pAP-1-Luc (A) or pSRE-Luc (B) together with 0.2 μg pRSV-lacZ with or without 0.9 μg MKP expression vectors. Eighteen hours later, cells were serum-starved for 12 h and then treated with or without 10 ng/ml PMA. Six hours after stimulation, cell lysates were obtained. For U0126 treatment, cells were exposed to drug for 1 h before stimulation. White bars represent luciferase activity compared to cells without PMA treatment (black bars). Data are means from three independent experiments.

characteristic of ERK cytoplasmic scaffold proteins [18]. It is likely that cytoplasmic retention prevents phospho-ERK from dephosphorylation by nuclear phosphatases, such as MKP-1 and MKP-2.

The data presented here is the first demonstration that MKP-7, a JNK phosphatase, plays a specific and negative role in ERK-dependent gene expression. Previously, we showed regulation of MKP-7 by post-translational modification: in quiescent cells MKP-7 levels remained low due to rapid turnover by ubiquitin-mediated proteolysis, but mitogen stimulation activated ERK and phosphorylated Ser-446 of MKP-7, stabilizing the protein [10]. Together with the present data, it is likely that upon stimulation with mitogen, MKP-7 accumulates and strongly suppresses ERK-dependent gene expression, which may lead to negative feedback by newly expressed MKP-1, -2 and -3, all of which are early response gene products.

MKP-7 has been mapped to 12p12, an area prone to deletions in childhood acute lymphoblastic leukemia and several solid neoplasms [20]. Clinical studies also demonstrate a high incidence of hemizygosity and low-expression of MKP-7 in lymphoblastic leukemia and prostate cancer [21,22]. Our data demonstrating that MKP-7 suppresses not only JNK but also the ERK cascade suggests that down-regulation of MKP-7 gene expression in cells may be critical for initiation or progression of some tumors.

Conclusion

Several lines of evidence presented here strongly suggest that MKP-7, a JNK phosphatase, inhibits ERK-dependent gene expression by blocking nuclear accumulation of phospho-ERK2. To our knowledge, this is the first demonstration that an MKP protein functions as an anchor protein rather than a phosphatase.

Acknowledgments

We thank Dr. K. Yamashita (Kanazawa University) for anti-FLAG antibody. We thank Dr. J. Magae (Institute of Research and Innovation, Kashiwa, Japan) and N.H. Heintz (University of Vermont, Burlington, VT) for providing us with pCMV-b-galactosidase. We thank Dr. M. Karin (University of California, San Diego) for pSRα-HA-ERK2. Thanks are also due to N. Sasaki for secretarial assistance. This work was supported in part by grants-in-aid for Scientific Research (B) provided by the Japan Society for the Promotion of Science (to H.S. and M.S.).

References

[1] L. Chang, M. Karin, Mammalian MAP kinase signalling cascades, Nature 410 (2001) 37–40.
[2] T. Wada, J.M. Penninger, Mitogen-activated protein kinases in apoptosis regulation, Oncogene 23 (2004) 2838–2849.
[3] L.O. Murphy, J. Blenis, MAPK signal specificity: the right place at the right time, Trends Biochem. Sci. 31 (2006) 268–275.
[4] M. Ebisuya, K. Kondoh, E. Nishida, The duration, magnitude and compartmentalization of ERK MAP kinase activity: mechanisms for providing signaling specificity, J. Cell Sci. 118 (2005) 2997–3002.
[5] D.M. Owens, S.M. Keyse, Differential regulation of MAP kinase signalling by dual-specificity protein phosphatases, Oncogene 26 (2007) 3203–3213.
[6] A. Theodosiou, A. Ashworth, MAP kinase phosphatases, Genome Biol. 3 (2002) 3009.1–3009.10.
[7] K. Masuda, H. Shima, M. Watanabe, K. Kikuchi, MKP-7, a novel mitogen-activated protein kinase phosphatase, functions as a shuttle protein, J. Biol. Chem. 276 (2001) 39002–39011.
[8] T. Tanoue, T. Yamamoto, R. Maeda, E. Nishida, Novel MAPK phosphatase MKP-7 acts preferentially on JNK/SAPK and p38 alpha and beta MAPKs, J. Biol. Chem. 276 (2001) 26629–26639.
[9] K. Masuda, H. Shima, C. Katagiri, K. Kikuchi, Activation of ERK induces phosphorylation of MAPK phosphatase-7, a JNK specific phosphatase, at Ser-446, J. Biol. Chem. 278 (2003) 32448–32456.
[10] C. Katagiri, K. Masuda, T. Urano, K. Yamashita, Y. Araki, K. Kikuchi, H. Shima, Phosphorylation of Ser-446 determines stability of MKP-7, J. Biol. Chem. 280 (2005) 14716–14722.
[11] T. Akagi, K. Sasai, H. Hanafusa, Refractory nature of normal human diploid fibroblasts with respect to oncogene-mediated transformation, Proc. Natl. Acad. Sci. USA 100 (2003) 13567–13572.
[12] T. Koda, S. Hasan, A. Sasaki, Y. Arimura, M. Kakinuma, Regulatory sequences required for hst-1 expression in embryonal carcinoma cells, FEBS Lett. 342 (1994) 71–75.
[13] A. Zuniga, J. Torres, J. Ubeda, R. Pulido, Interaction of mitogen-activated protein kinases with the kinase interaction motif of the tyrosine phosphatase PTP-SL provides substrate specificity and retains ERK2 in the cytoplasm, J. Biol. Chem. 274 (1999) 21900–21907.
[14] R. Pulido, A. Zuniga, A. Ullrich, PTP-SL and STEP protein tyrosine phosphatases regulate the activation of the extracellular signal-regulated kinases ERK1 and ERK2 by association through a kinase interaction motif, EMBO J. 17 (1998) 7337–7350.
[15] J.J. Murioz, C. Blanco-Aparicio, R. Pulido, Differential interaction of the tyrosine phosphatases PTP-SL, STEP and HePTP with the mitogen-activated protein kinases ERK1/2 and p38alpha is determined by a kinase specificity sequence and influenced by reducing agents, Biochem. J. 15 (2003) 193–201.
[16] M. Karlsson, J. Mathers, R.J. Dickinson, M. Mandl, S.M. Keyse, Both nuclear-cytoplasmic shuttling of the dual specificity phosphatase MKP-3 and its ability to anchor MAP kinase in the cytoplasm are mediated by a conserved nuclear export signal, J. Biol. Chem. 279 (2004) 41882–41891.
[17] M. Mandl, D.N. Slack, S.M. Keyse, Specific inactivation and nuclear anchoring of extracellular signal-regulated kinase 2 by the inducible dual-specificity protein phosphatase DUSP, Mol. Cell. Biol. 25 (2005) 1830–1845.
[18] E. Formstecher, J.W. Ramos, M. Fauquet, D.A. Calderwood, J.C. Hsieh, B. Canton, X.T. Nguyen, J.V. Barnier, J. Camonis, M.H. Ginsberg, H. Chneiweiss, PEA-15 mediates cytoplasmic sequestration of ERK MAP kinase, Develop. Cell 1 (2001) 239–250.
[19] S. Torii, M. Kusakabe, T. Yamamoto, M. Maekawa, E. Nishida, Sef is a spatial regulator for Ras/MAP kinase signaling, Develop. Cell 7 (2004) 33–44.
[20] I. Hoornaert, P. Marynen, J. Goris, R. Sciot, M. Baens, MAPK phosphatase DUSP16/MKP-7, a candidate tumor suppressor for chromosome region 12p12-13, reduces BCR-ABL-induced transformation, Oncogene 22 (2003) 7728–7736.
[21] A. Montpetit, J. Larose, G. Boily, S. Langlois, N. Trundel, D. Sinnett, Mutational and expression analysis of the chromosome 12p candidate tumor suppressor genes in pre-B acute lymphoblastic leukemia, Leukemia 18 (2004) 1499–1504.
[22] A.S. Kibel, J. Huagen, C. Guo, W.B. Isaacs, Y. Yan, K.J. Pienta, P.J. Goodfellow, Expression mapping at 12p12-13 in advanced prostate carcinoma, Int. J. Cancer 109 (2004) 668–672.

J Neurooncol (2010) 100:43–49
DOI 10.1007/s11060-010-0147-3

LABORATORY INVESTIGATION - HUMAN/ANIMAL TISSUE

CDC25A mRNA levels significantly correlate with Ki-67 expression in human glioma samples

Yoji Yamashita · Isao Kasugai · Masami Sato · Nobuhiro Tanuma · Ikuro Sato · Miyuki Nomura · Katsumi Yamashita · Yukihiko Sonoda · Toshihiro Kumabe · Teiji Tominaga · Ryuichi Katakura · Hiroshi Shima

Received: 4 December 2009 / Accepted: 15 February 2010 / Published online: 10 March 2010

Abstract Cell division cycle 25 (CDC25) phosphatases are cell-cycle regulatory proteins which are overexpressed in a significant number of human cancers. This study evaluated the role of CDC25 phosphatases in human glioma proliferation. Upregulation of CDC25A was observed in human glioma specimens and human glioma cell lines. Comparison of expression levels of CDC25A and CDC25B messenger ribonucleic acid (RNA) to Ki-67 labeling index in glioma tissues found that Ki-67 labeling index was significantly correlated with the expression of CDC25A, but not with that of CDC25B. Depletion of CDC25A by small interfering RNA and inhibition of CDC25 suppressed cell proliferation and induced apoptosis in glioma cell lines, indicating that CDC25A is a potential target for the development of new therapy for glioma.

Keywords CDC25A · Glioma · Ki-67 · Protein phosphatase

Yoji Yamashita and Isao Kasugai contributed equally to this work.

Y. Yamashita · I. Kasugai · M. Sato · N. Tanuma · M. Nomura · H. Shima (✉)
Division of Cancer Chemotherapy, Miyagi Cancer Center Research Institute, 47-1 Nodayama, Medeshima-Shiode, Natori, Miyagi 981-1293, Japan
e-mail: shima-hi632@pref.miyagi.jp

Y. Yamashita · R. Katakura
Department of Neurosurgery, Miyagi Cancer Center, Natori, Miyagi, Japan

I. Sato
Section of Clinical Research, Miyagi Cancer Center Research Institute, Natori, Miyagi, Japan

K. Yamashita
Division of Life Science, Graduate School of Natural Science and Technology, Kanazawa University, Kanazawa, Ishikawa, Japan

Y. Sonoda · T. Kumabe · T. Tominaga
Department of Neurosurgery, Tohoku University Graduate School of Medicine, Sendai, Miyagi, Japan

Introduction

Glioblastomas are the most common and lethal type of malignant brain tumor. Median survival from the time of diagnosis is less than a year, with fewer than 5% of patients surviving 5 years. Glioblastoma is characterized by highly proliferative and invasive activity, and widespread infiltration of tumor cells into the surrounding brain tissue [1]. Recent standard therapy for glioblastomas includes surgical resection, radiotherapy, and adjuvant temozolomide chemotherapy administered both during and after radiotherapy. However, most patients develop tumor recurrence or progression after this multimodality treatment. There is clearly an urgent need to develop new classes of treatment modalities, such as molecular target-directed therapies [2–4]. Understanding the molecular pathogenesis of glioma may allow the rational development of new therapy approaches.

The rate of cell proliferation in glioma tissues as assessed by Ki-67 immunoreactivity has been studied as a prognostic indicator, and correlates with tumor grade and clinical course [5, 6]. Ki-67 detected by MIB-1 antibody is a core antigen present in proliferating cells and absent in quiescent cells. This antigen is expressed in all phases of the cell cycle except for G0 and the early parts of G1. The precise function of the Ki-67 protein is still unclear. Therefore, identification of molecules involved in the upregulation of Ki-67 antigen may help to understand the

malignant phenotype of glioma, and may become a candidate target for treatment.

Regular control of cell cycle progression requires correct function of a small family of phosphatases termed cell division cycle 25 (CDC25), which contain highly conserved domains for dual specificity phosphatases [7]. The CDC25 family is fundamental in transitions between cell cycle phases during normal cell division through the activation of cyclin-dependent kinase (CDK)/cyclin complexes. Three genes code for the CDC25A, B, and C proteins with both different and redundant specificities and regulations in humans. In particular, the CDC25A and B phosphatases have oncogenic properties and are overexpressed singly in some types of cancers and together in others [8]. Therefore, CDC25s are promising targets for the development of new anticancer therapeutic strategies. Overexpression of CDC25 is linked to clinicopathological features such as tumor grade, recurrent disease, or disease-free survival [9, 10].

The present study examined whether CDC25 isotype-specific linkage is present in human glioblastoma samples.

Materials and methods

Patients and glioma samples

Newly diagnosed human glioma tissues were obtained from 25 consecutive patients (15 males and 10 females) who underwent surgery (14 surgical resections and 11 stereotactic biopsies) at the Department of Neurosurgery, Miyagi Cancer Center, from July 2008 onwards. Their median age was 63 years (range 21–83). Without regard to tumor volumes or tumor malignancies, small samples weighing from 10 to 30 mg were collected for this study from all surgical specimens and serial numbers were added in the order of surgery. Each sample was immediately divided in two. One was frozen for ribonucleic acid (RNA) preparation, the other was formalin-fixed and paraffin-embedded for conventional histopathological evaluation and counting of Ki-67 labeling index (Ki-67LI). Histological diagnoses were made by a neuropathologist, based on the World Health Organization criteria as glioblastoma (16 cases; nos. 1–5, 7–12, 14, 18–21), anaplastic astrocytoma (6 cases; nos. 6, 13, 17, 23–25), and diffuse astrocytoma (3 cases; nos. 15, 16, 22). RNA analysis was approved by the Ethics Committee of the Miyagi Cancer Center.

Quantitative real-time polymerase chain reaction

Total RNA was prepared from the specimens with the RNeasy Lipid Mini kit (Qiagen). Complementary deoxyribonucleic acid (cDNA) was synthesized using an oligo-d(T)12-18 primer with Superscript III reverse transcriptase (Invitrogen) and applied to quantitative real-time polymerase chain reaction (qPCR) using the LightCycler 480 and the probes master kit (Roche Diagnostics). The PCR primers and the probes were designed and selected for the intron spanning condition according to the online software (Roche Applied Science). The PCR reaction was performed in 20 μl containing 10 μl of Probes Master (Roche), 0.5 μM of each primer, 0.1 μM of probe, and 5 μl of cDNA solution. The protocol of PCR involved initial denaturation at 95°C for 5 min, followed by 55 cycles of 95°C for 10 s, then 60°C for 25 s. Threshold cycle values (Second Derivative Maximum method) were normalized to the housekeeping gene, porphobilinogen deaminase (PBGD). Human brain (frontal lobe) total RNA from a pool of four different donors and from single donor were obtained from Clontech (Palo Alto, CA, USA) and BioChain Institute (Hayward, CA), respectively, were also subjected to cDNA synthesis and subsequent qPCR. The levels of CDC25A and CDC25B messenger RNA (mRNA) in the gliomas were expressed as ratios to that of the mixed human brain RNA sample (Clontech). The following probes were used: no. 17 (CDC25A), no. 68 (CDC25B), no. 2 (CDC25C), and no. 25 (PBGD) (Roche Universal Probe Library). The primer sequences were as follows: CDC25A 5′-TCTGAAGAATGAGGAGGAGACC-3′ and 5′-AAACAGCTTGCATCGGTTGT-3′; CDC25B 5′-ACG CCCGTGCAGAATAAG-3′ and 5′-AGTGATTTTGAG CGGAGGAC-3′; CDC25C 5′-GAGGCCATGTCGGAA GAAG-3′ and 5′-GCTTCCTTCCTCTCTTGTGG-3′; PBGD 5′-AGCTATGAAGGATGGGCAAC-3′ and 5′-TTGTATG CTATCTGAGCCGTCTA-3′.

Ki-67LI

Ki-67LI was measured. Fields with the highest number of Ki-67-labeled cells were initially selected through generalized survey, and then the percentage of positive-labeled cells was determined by counting more than 1,000 tumor nuclei of more than three fields of a specimen at ×400 magnification without knowing any clinical information. Only strong nuclear staining was regarded as positive, and weak nuclear or cytoplasmic staining was regarded as negative.

Statistical analysis

Statistical analysis used the software Statview 5.0 (SAS Institute, Cary, NC). The expression level of CDC25A mRNA was compared with the Ki-67LI in human primary glioblastoma samples using simple linear regression analysis, and a P value of less than 0.05 was considered to indicate statistical significance.

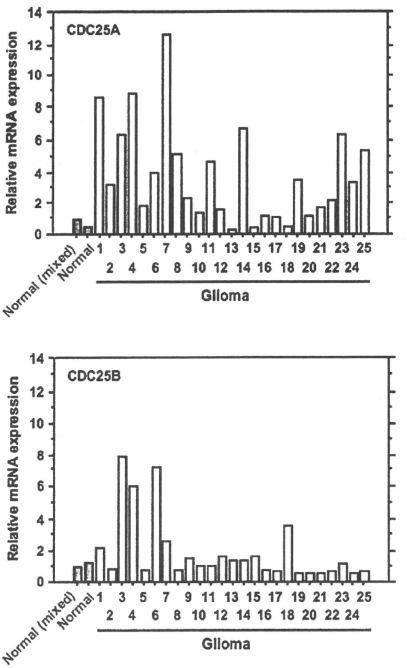

Fig. 1 Analysis of *CDC25A* and *CDC25B* mRNA levels in human glioma samples. Expression levels of *CDC25A* (*upper*) or *CDC25B* (*lower*) mRNA in normal brain and primary glioblastoma samples were estimated by qPCR. Results were normalized to the mRNA levels of the housekeeping gene porphobilinogen deaminase (PBGD) and shown relative to mRNA levels seen in the normal brain (four mixed samples), which was set as 1.0

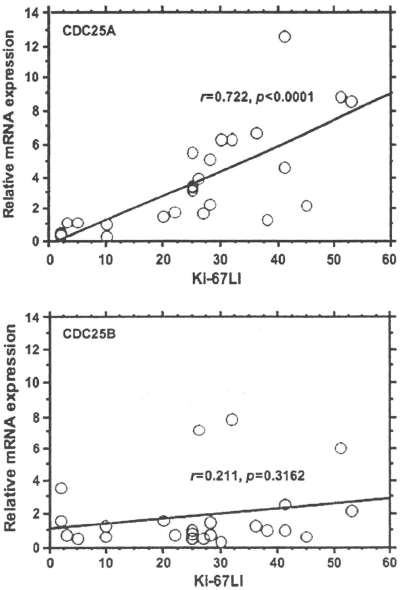

Fig. 2 Statistical comparison of the expression levels of *CDC25A* and *CDC25B* mRNA with *Ki-67LI* in human primary glioma samples. Simple linear regression analysis showed the relationship between the expression of *CDC25A* (*upper*) or *CDC25B* (*lower*) mRNA and *Ki-67LI* in human primary glioblastoma samples

Cell culture

Human glioblastoma cell line A172 was obtained from the RIKEN BRC (Tsukuba, Ibaraki, Japan), and U87, U251, and U373 were obtained from DS PHARMA Biomedical (Osaka, Japan), Health Science Research Resources Bank (Osaka, Japan), and ATCC, respectively. A172, U87, U251, and U373 cells were maintained in Dulbecco's modified Eagle's medium supplemented with 10% fetal bovine serum (FBS). A172 cells were cultured in RPMI-1640 (Gibco) supplemented with 10% FBS. Normal human astrocytes (NHAs) (Lonza, Basel, Switzerland) were cultured in Astrocyte Basal Medium supplemented with AGM SingleQuots according to the manufacturer's instructions. NHA proliferation was arrested after 21 days culture, and used as quiescent cells.

Small interfering RNA transfection

Small interfering RNA (siRNA) duplexes against human CDC25A (Stealth RNAi), HSS101654 (siRNA1-CDC25A), and HSS10165 (siRNA2-CDC25A) were purchased from Invitrogen. Stealth RNAi Negative Control Medium GC duplex (Invitrogen) was used as the control. siRNA transfection was undertaken using Lipofectamine RNAiMAX (Invitrogen) according to the manufacturer's instruction at a final siRNA concentration of 5 nM in the culture.

Cell proliferation assay

Cells transfected with siRNA or small compounds were plated on a 96-well plate in octuplicate wells. Cell

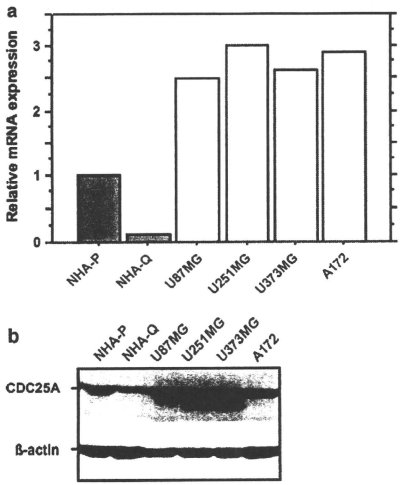

Fig. 3 Analyses of CDC25A mRNA levels (**a**) and protein levels (**b**) in human glioma cell lines. **a** Expression levels of CDC25A mRNA in normal human astrocytes in the proliferating (*NHA-P*) and quiescent stages (*NHA-Q*) and glioma cell line samples were estimated by qPCR. Results were normalized to the mRNA levels of the housekeeping gene porphobilinogen deaminase (PBGD) and shown relative to the mRNA levels seen in normal brain (four mixed samples), which was set as 1.0. **b** Immunoblot analysis of *CDC25A* in normal human astrocytes and glioma cell lines

proliferation was assessed as incorporation of 1-methoxy PMS by the DOJINDO cell counting Kit-8 according to the manufacture's protocol (DOJINDO, Kumamoto, Japan). Optical density was read at 450 nm at various time points using a microplate reader (TECAN, Research Triangle Park). The corresponding background value was subtracted from the reading obtained from each well. To estimate half maximal inhibitory concentration (IC50) for each compound, values at 96 h of treatment were used for linear regression analysis.

Caspase-3 and -7 activity

To measure apoptosis in glioma cell lines treated with siRNAs or small compounds, the cells were plated on a 96-well plate in triplicate wells. The caspase-3 and -7 enzyme activities were measured by the Caspase-Glo 3/7 Assay (Promega) according to the manufacturer's protocol.

Results

Upregulation of CDC25A in human glioma samples

The expression level of the three CDC25 family members (CDC25A, B, and C) was examined in 25 human glioma samples by qPCR. Figure 1 shows the mRNA levels of CDC25A and CDC25B in the glioma samples compared to that in normal (mixed) brain. The CDC25A and CDC25B mRNAs were elevated in 17 (68%) and 6 (24%), respectively, of these samples. In contrast, the CDC25C mRNA level was under the detection limit in the normal brain, and no induction was observed in tumor samples.

Correlation of CDC25A expression with Ki-67LI

To examine the possible involvement of CDC25A and CDC25B in cellular proliferation, the expression of Ki-67, a marker for cell proliferation, was examined by immunohistochemistry with MIB-1 antibody. Figure 2 shows that Ki-67LI levels were significantly correlated with the level of CDC25A ($r = 0.722$, $P < 0.0001$), but not with that of CDC25B ($r = 0.211$, $P = 0.3162$). Therefore, overexpression of CDC25A rather than CDC25B is involved in increased cell proliferation in glioma tissues.

Upregulation of CDC25A in human glioma cell lines

CDC25A expression was examined in 4 glioma cell lines, U87MG, U251MG, U373MG, and A172. NHAs in the proliferating and quiescent stages were used as controls. Figure 3a shows the relative expression of CDC25A in these cells. The level of CDC25A mRNA was reduced to 20% after the end of proliferation in NHAs, supporting the importance of CDC25A expression in cell proliferation. Compared to proliferating NHAs, glioma cell lines such as U87MG, U251MG, U373MG, and A172 showed 2- to 3-fold increase in CDC25A mRNA expression. Analysis of the CDC25A protein levels in these cells showed almost similar levels to those of CDC25A mRNA (Fig. 3b). Therefore, CDC25A is overexpressed in glioma cell lines.

Inhibitor of CDC25 suppresses cell proliferation

To examine the role of CDC25s in glioblastoma, the effects of two quinone-based CDC25 inhibitors, BN82002 [11] and BN82685 [12], were analyzed on cell proliferation in U87MG and A172 cells (Fig. 4a). Both compounds inhibited CDC25A and CDC25B, and they were already reported to be active not only in vitro but also in vivo [11, 12]. U87MG and A172 cells were treated with increasing concentrations of the inhibitors until 96 h. The IC50s of

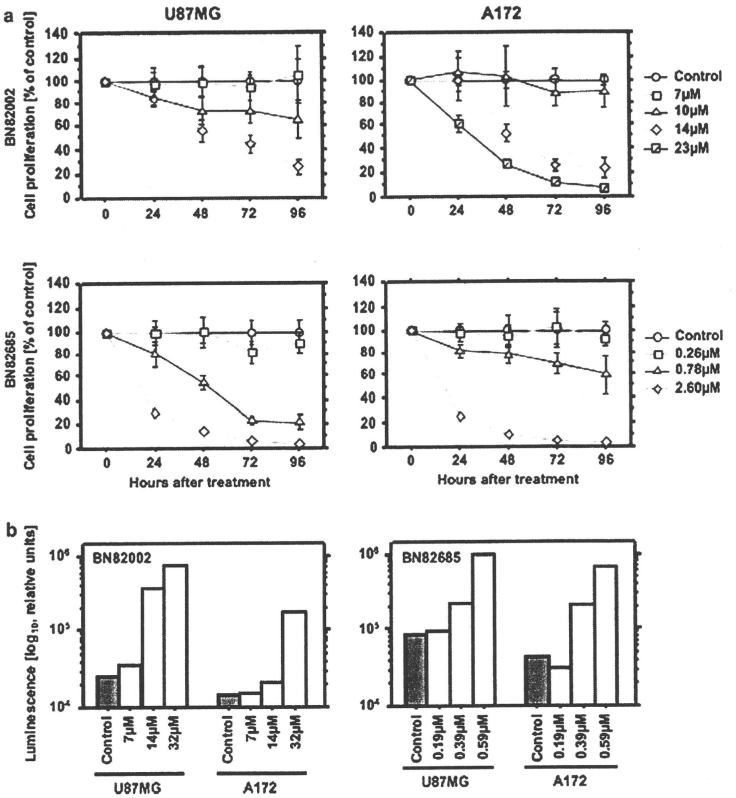

Fig. 4 Inhibition of CDC25 reduces cell proliferation (**a**) and induces cell apoptosis (**b**). *U87MG* and *A172* cells were grown in 98-well plates and treated with dimethyl sulfoxide (*control*) or CDC25 inhibitors, *BN82002* or *BN82685*. Cell proliferation assay (**a**) and caspase-3 and -7 assay (**b**) as described in "Materials and methods"

BN82002 for U87MG and A172 were 18 and 12 μM, respectively, and the IC50s of BN82685 for U87MG and A172 were 0.54 and 0.90 μM, respectively. In addition, BN82002 and BN82685 dose-dependently induced apoptosis, as assessed by the caspase-3 and -7 activities (Fig. 4b).

Silencing of CDC25A inhibits cell growth

To evaluate the CDC25A specific role in proliferation and survival in glioma cells, the siRNA approach was used to deplete CDC25A in the glioma cell lines. Two CDC25A-specific siRNA (siRNA1-CDC25A and siRNA2-CDC25A) and negative control siRNA were transfected into U87MG and A172 cells, both of which overexpressed CDC25A. Immunoblot analysis confirmed suppression of CDC25A expression in siRNA1-CDC25A and siRNA2-CDC25A at days 2 and 3 after transfection (Fig. 5a).

The effects of CDC25A suppression on the cell proliferation of the glioma cells were analyzed. U87MG and A172 were transfected with siRNA1-CDC25A, siRNA2-CDC25A, or control siRNA, and cell proliferation was assessed daily over 5 days (Fig. 5b). Both cell lines

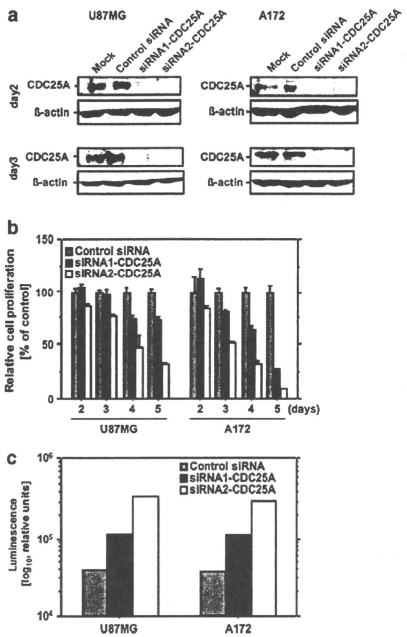

Fig. 5 Suppression of CDC25A by siRNA treatment inhibits cell proliferation and induces apoptosis in glioma cells. *U87MG* and *A172* cells were transfected with control siRNA or siRNAs against human CDC25A as described in "Materials and methods" and cultured for the indicated times. The cells were lysed and immunoblot was performed using antibody for CDC25A or β-actin (**a**). Cell proliferation assay (**b**) and caspase-3 and -7 assay (**c**) as described in "Materials and methods"

transfected with siRNA1-CDC25A and siRNA2-CDC25A showed slower growth rates than cells transfected with control siRNA. Additionally, caspase activity was measured in the CDC25A-depleted cells. The U87MG and A172 cells transfected with the CDC25A siRNAs showed increased levels of caspase, demonstrating that apoptosis was induced in the CDC25A-depleted cells (Fig. 5c). Therefore, CDC25A-mediated cell proliferation and survival in glioma cells, and suppression resulted in growth inhibition.

Discussion

The present study investigated expression levels of CDC25s in human gliomas, and found that CDC25A is overexpressed, and that its expression level is closely correlated with Ki-67LI in gliomas. This may be the first functional molecule with expression well correlated with Ki-67LI in glioma tissues.

CDC25 was overexpressed and contributed to tumorigenesis in various patients with high-grade malignant tumor [8]. Both CDC25 A and B have prognostic value. Overexpression of CDC25B and significant correlation of expression with shorter periods of disease-free survival were found in glioma samples, but the level of CDC25A expression was not defined [13]. CDC25 overexpression within each cancer subtype tends to occur in an isoform-specific manner, and the overexpression of multiple isoforms in the same cancer subtypes probably occurs through independent pathways [8].

This study showed that expression of CDC25A was more prominent and correlated better with Ki-67LI than expression of CDC25B in glioma tissues. These findings indicate that overexpression of CDC25A rather than CDC25B is involved in increased cell proliferation in glioma tissues. The majority of studies have clearly shown the prognostic importance of Ki-67LI in glioma, both regarding survival and recurrence [5, 6], so CDC25A should be considered the marker for prognosis and/or target for treatment rather than CDC25B.

The present study showed overexpression of CDC25A in both surgical specimens and glioma cell lines. CDC25A expression was 2–3 times higher in glioma cell lines than the proliferating NHAs, suggesting overexpression of CDC25A characterizes the malignant phenotype of glioma cells. The mechanisms by which CDC25 isoforms become deregulated during tumorigenesis remains unclear. Several positive and/or negative regulators of CDC25A transcription have been described, including c-myc, hypoxia-inducible factor-1 alpha, p53, p21, and E2F, but there is no evidence that CDC25 overexpression resulted from gene amplification or rearrangements, or any other specific genetic mutations that may be responsible for deregulating CDC25 activities in cancer [8]. The development of CDC25A targeting therapy will require further studies to reveal the CDC25 biology in glioma.

Recently, CDKs are crucial in the control of the cell cycle, so are attractive pharmacological targets for the development of antiproliferative agents. Inhibitors of these enzymes are currently in clinical trials in patients with various malignant tumors. CDC25s are activators of CDKs, so are particularly attractive target candidates for the development of anticancer agents. Various classes of CDC25 inhibitors have been identified, and the specificities were examined in vitro. We selected BN82002 and BN82685 because of their relatively higher selectivity for CDC25A. The IC50s of BN82002 towards CDC25A, CDC25B2, and CDC25B3 are 2.4, 3.9, and 6.3 μM, and

those of BN82685 are 109, 160, and 249 nM, respectively, in vitro [11, 12]. In this study, these inhibitors showed remarkable growth suppression and induction of apoptosis in glioma cells, and similar effects were observed after selective depletion of CDC25A from glioma cells by siRNA. These results suggest that CDC25A is important in glioma cell proliferation and survival, and CDC25A targeted therapy using isoform specific inhibitor is a potential approach to glioma therapy.

Acknowledgments This work was supported in part by Grants-in-aid for Scientific Research (C) to Y.Y. and H.S. and for Exploratory Research to R.K. provided by the Japan Society for the Promotion of Science.

References

1. Ohgaki H, Kleihues P (2007) Genetic pathways to primary and secondary glioblastoma. Am J Pathol 170:1445–1453
2. Sathornssumetee S, Reardon DA, Desjardins A, Quinn JA, Vredenburgh JJ, Rich JN (2007) Molecularly targeted therapy for malignant glioma. Cancer 110:13–24
3. Parsons DW, Jones S, Zhang X, Lin JC, Leary RJ, Angenendt P, Mankoo P, Carter H, Siu IM, Gallia GL, Olivi A, McLendon R, Rasheed BA, Keir S, Nikolskaya T, Nikolsky Y, Busam DA, Tekleab H, Diaz LA Jr, Hartigan J, Smith DR, Strausberg RL, Marie SK, Shinjo SM, Yan H, Riggins GJ, Bigner DD, Karchin R, Papadopoulos N, Parmigiani G, Vogelstein B, Velculescu VE, Kinzler KW (2008) An integrated genomic analysis of human glioblastoma multiforme. Science 321:1807–1812
4. Rich JN, Hans C, Jones B, Iversen ES, McLendon RE, Rasheed BK, Dobra A, Dressman HK, Bigner DD, Nevins JR, West M (2005) Gene expression profiling and genetic markers in glioblastoma survival. Cancer Res 65:4051–4058
5. Faria MH, Gonçalves BP, do Patrocínio RM, de Moraes-Filho MO, Rabenhorst SH (2006) Expression of Ki-67, topoisomerase IIalpha and c-MYC in astrocytic tumors: correlation with the histopathological grade and proliferative status. Neuropathology 26:519–527
6. Johannessen AL, Torp SH (2006) The clinical value of Ki-67/MIB-1 labeling index in human astrocytomas. Pathol Oncol Res 12:143–147
7. Boutros R, Dozier C, Ducommun B (2006) The when and wheres of CDC25 phosphatases. Curr Opin Cell Biol 18:185–191
8. Boutros R, Lobjois V, Ducommun B (2007) CDC25 phosphatases in cancer cells: key players? Good targets? Nat Rev Cancer 7:495–507
9. Kiyokawa H, Ray D (2008) In vivo roles of CDC25 phosphatases: biological insight into the anti-cancer therapeutic targets. Anticancer Agents Med Chem 8:826–832
10. Lazo JS, Wipf P (2008) Is Cdc25 a druggable target? Anticancer Agents Med Chem 8:837–842
11. Brezak MC, Quaranta M, Mondésert O, Galcera MO, Lavergne O, Alby F, Cazales M, Baldin V, Thurieau C, Harnett J, Lanco C, Kasprzyk PG, Prevost GP, Ducommun B (2004) A novel synthetic inhibitor of CDC25 phosphatases: BN82002. Cancer Res 64:3320–3325
12. Brezak MC, Quaranta M, Contour-Galcera MO, Lavergne O, Mondesert O, Auvray P, Kasprzyk PG, Prevost GP, Ducommun B (2005) Inhibition of human tumor cell growth in vivo by an orally bioavailable inhibitor of CDC25 phosphatases. Mol Cancer Ther 4:1378–1387
13. Nakabayashi H, Hara M, Shimizu K (2006) Prognostic significance of CDC25B expression in gliomas. J Clin Pathol 59:725–728

ACTA CYTOLOGICA

Acta Cytologica 2011;55:173–179
DOI: 10.1159/000320860

Received: December 16, 2009
Accepted: December 22, 2009
Published online: February 15, 2011

Cytological Characteristics of Pulmonary Pleomorphic and Giant Cell Carcinomas

Kenzo Hiroshima[a, b] Hirotoshi Dosaka-Akita[a] Katsuo Usuda[a] Shigeaki Ogura[a] Yoko Kusunoki[a] Tetsuro Kodama[a] Yasuki Saito[a] Masami Sato[a] Yutaka Tagawa[a] Masayuki Baba[a] Takashi Hirano[a] Takeshi Horai[a] Yoshihiro Matsuno[a]

[a]Committee on Pulmonary Cytology, The Japan Lung Cancer Society, Chiba,
[b]Department of Pathology, Tokyo Women's Medical University Yachiyo Medical Center, Yachiyo, Japan

Key Words
Cytology · Giant cell carcinoma · Lung neoplasms · Pleomorphic carcinoma · Sarcomatoid carcinoma

Abstract
Objective: To establish cytological features of pulmonary pleomorphic carcinoma (PC) or giant cell carcinoma (GC), we evaluated the cytological characteristics of these tumors using a multidisciplinary approach. ***Study Design:*** Samples from 13 surgically resected and histologically confirmed PC or GC patients were collected from our institutes. Eight cases without prior chemotherapy before surgery were selected, and cytological features were analyzed. ***Results:*** The background contained numerous lymphocytes and neutrophils. The tumor cells were arranged in flat loose clusters, but some were in fascicles. The shape of the tumor cell was spindle or pleomorphic, and the sizes of the tumor cells varied by more than 5-fold. The tumor cells had an abundant, thick and well-demarcated cytoplasm. The location of the nucleus was centrifugal, and the nucleus was oval or irregularly shaped. Multinucleated giant cells were frequently observed. The size of the nucleus was more than 5 times that of normal lymphocytes, and its size also varied by more than 5-fold. The nuclear membrane was thin, and nuclear chromatin was coarsely granular, while the nucleolus was single and round. ***Conclusion:*** PC or GC has characteristic cytological features, however, spindle cells tended to be hardly observed in cytological specimens in some cases.

Pleomorphic carcinoma (PC) is defined as a poorly differentiated non-small cell lung carcinoma (NSCLC), namely squamous cell carcinoma, adenocarcinoma or large cell carcinoma containing spindle cells and/or giant cells, or a carcinoma containing only spindle cells and giant cells [1]. The spindle or giant cell component should comprise at least 10% of the tumor. Giant cell carcinoma (GC) is NSCLC composed of highly pleomorphic mono- and/or multinucleated tumor giant cells. This tumor is composed entirely of giant cells and does not have specific patterns of adenocarcinoma, squamous cell or large-cell carcinoma. The tumor cells are discohesive and tend to dissociate from each other [1].

The prognosis for PC patients is worse than that for patients with other NSCLC in surgically operated cases [2–4]. However, there have been some contradictory reports that PC has similar clinical behavior and prognosis as other NSCLC [5–7]. Histologic diagnosis is usually

KARGER

Fax +41 61 306 12 34
E-Mail karger@karger.ch
www.karger.com

0001–5547/11/0552–0173$38.00/0

Accessible online at:
www.karger.com/acy

Correspondence to: Dr. Kenzo Hiroshima
Department of Pathology
Tokyo Women's Medical University Yachiyo Medical Center
477-96 Owada-Shinden, Yachiyo-shi, Chiba 276-8524 (Japan)
Tel. +81 47 450 6000, Fax +81 47 458 7047, E-Mail kenzo@tymc.twmu.ac.jp

Table 1. Clinical summary of cases with pleomorphic carcinoma or giant cell carcinoma

Case	Age/ sex	Location	Smoking pack-years	Size mm	Stage	Adjuvant therapy	Follow up		Compo-nent
							months	prognosis	
1	69/F	LU/P	49	17		none	14	alive	S/G/A/L
2	76/M	LU/P	122	55	IIIA	chemo. + rad.	7	alive	S/G/A/L
4	62/M	RU/P	126	80	IV	none	3.5	dead	S/A
7	68/M	LL/P	18	16	IA	none	32	recurrence	S/G/A
8	68/M	LL/P	50	32	IIB	none	21	recurrence	S/A
9	82/M	RM/P	60	60	IIB	none	60	alive	S/G
10	39/F	LL/C	8	50	IIIA	rad. + chemo.	40	alive	S/G/A
12	78/M	RU/P	55	25	IV	UFT	23	alive	G

LU = Left upper lobe; RU = right upper lobe; LL = left lower lobe; RM = right middle lobe; P = peripheral; C = central; S = spindle cells; G = giant cells; A = adenocarcinoma; L = large cell carcinoma; Chemo. = chemotherapy; Rad. = radiotherapy; UFT = 5-fluoro-uracil derivative.

made with surgically removed tumors; however, diagnosis has to be made based on small biopsies or cytological specimens for patients with an advanced-stage tumor. Because of the difficulty in making a definite diagnosis of PC or GC, it is not clear whether the prognosis of patients with those tumors in the advanced stage is worse than that for patients with other NSCLCs. Although cytological findings of PC or GC have been documented in a few reports [8–13], there have been no multi-institutional studies carried out by pulmonary cytopathologists. The aim of this study was to elucidate the cytological characteristics of PC or GC with specimens obtained from the touch imprints of surgically removed tumors or pre-operative transbronchial cytology specimens in patients whose tumor was surgically removed and confirmed histologically to be PC or GC, and to extend application of those findings to specimens obtained from brushing or curettage of advanced-stage tumors.

Materials and Methods

We collected 16 resected tumors that were identified as PC or GC from our own institutes or from consultation cases. Pathological findings were reviewed by 3 pulmonary pathologists (K.H., T.K., and Y.M.), after which 13 of the tumors were diagnosed as PC or GC. Members of the Committee on Pulmonary Cytology of the Japan Lung Cancer Society evaluated the findings of their own original cytological and pathological specimens using a microscope and made digital images of representative microscopic findings for the 13 selected tumors. The digital images were copied to a CD and distributed to each member of the committee. Autopsy cases and patients who received chemotherapy before surgery were eliminated from this study, and 8 cases were selected for analyses of cytological features. All of the authors are experienced pulmonary cytopathologists with Board Certification from the Japanese Society of Clinical Cytology, and all are members of the Committee on Pulmonary Cytology of the Japan Lung Cancer Society.

Each member of the Committee on Pulmonary Cytology evaluated the cytological findings of the samples independently. We defined sarcomatoid component of PC as malignant giant and/or spindle cells. We defined epithelial component of PC as malignant tumor cells with glandular or squamous differentiation. Component of large-cell carcinoma is also included in epithelial component of PC. We defined large-cell carcinoma component as tumor cells which have a tendency to form loosely structured clusters composed of cells of unequal sizes without glandular or squamous differentiation. We evaluated cytological features of sarcomatoid component in each of the cases using the following parameters of the tumor cells by light microscopy: component of tumor cells, background, number, sizes of clusters, nuclear overlapping, arrangement, shape, size, variability in size, pleomorphism, surface, adhesion, color of the cytoplasm, nature of the cytoplasm, nuclear to cytoplasmic ratio, localization of the nucleus (centrifugal or peripheral), shape of the nucleus, size of the nucleus, pleomorphism of the nucleus, nuclear membrane, amount of chromatin, chromatin texture, distribution of chromatin, size and shape of the nucleolus, and number of nucleoli in the nucleus.

The age of the patients ranged from 39 to 82 years old (mean 67.8 years). Six were men and 2 were women. The tumor existed at the periphery of the lung in 7 cases and at the central part of the lung in 1 case. All of the patients were smokers. They smoked from 8 to 126 pack-years (average 61 pack-years). The size of the tumor was from 16 to 80 mm in diameter (average 42 mm). Lobectomy with lymph node dissection was performed in 7 cases, and partial resection of the lung without lymph node dissection was done in 1 case because of poor pulmonary function (case 1). The tumor stages were IA in 1 case, IIB in 2 cases, IIIA in 2 cases, and IV in 2 cases. The TNM classification of case 1 is T1NXMX (table 1).